



ELSEVIER

Journal of Alloys and Compounds 330–332 (2002) 752–759

Journal of
ALLOYS
AND COMPOUNDS

www.elsevier.com/locate/jallcom

High catalytic activity disordered VTiZrNiCrCoMnAlSn hydrogen storage alloys for nickel–metal hydride batteries

M.A. Fetcenko*, S.R. Ovshinsky, K. Young, B. Reichman, C. Fierro, J. Koch, F. Martin, W. Mays, T. Ouchi, B. Sommers, A. Zallen

Energy Conversion Devices/Ovonic Battery Company, 1707 Northwood Drive, Troy, MI 48084, USA

Abstract

Multielement, multiphase disordered metal hydride alloys have enabled the widespread commercialization of NiMH batteries by allowing high capacity and good kinetics while overcoming the crucial barrier of unstable oxidation/corrosion behavior to obtain long cycle life. Atomic engineering is used to promote a high concentration of active hydrogen storage sites vital for raising NiMH specific energy to 100 Wh kg^{-1} by utilizing metal hydride materials having in excess of 440 mAh g^{-1} specific capacity. New commercial applications demand fundamentally higher specific power and discharge rate kinetics. Disorder at the metal/electrolyte interface has enabled a surface oxide with metallic nickel alloy inclusions having a diameter less than 70 \AA embedded within the oxide, which provide exceptional catalytic activity to the metal hydride electrode surface and allowed NiMH specific power exceeding 1000 W kg^{-1} . © 2002 Elsevier Science B.V. All rights reserved.

Keywords: Metal hydride; Disorder; Surface catalysis

1. Introduction

Nickel–metal hydride (NiMH) batteries are in high volume commercial production for small portable battery applications, beginning in 1989 and achieving over 900 million annual worldwide cell production in 1999 [1]. The driving force for the rapid growth of NiMH is both technical and environmental, with energy and performance advantages over nickel–cadmium fueling the explosive growth of portable electronic devices such as communication equipment and laptop computers.

NiMH batteries have become the dominant advanced battery technology for electric vehicle (EV) and hybrid electric vehicle (HEV) applications by having the best overall performance in the wide-ranging requirements set by automotive companies. In addition to the essential performance targets of energy, power, cycle life and operating temperature, the following features of NiMH have established the technology preeminence:

- Flexible cell sizes from 60 mAh–250 Ah;
- Safe operation at high voltage (320+ volts);
- Excellent volumetric energy and power, flexible vehicle packaging;

- Easy application to series and series/parallel strings;
- Choice of cylindrical or prismatic cells;
- Safety in charge and discharge, including tolerance to abusive overcharge and overdischarge;
- Maintenance free;
- Excellent thermal properties;
- Capability to utilize regenerative braking energy;
- Simple and inexpensive charging and electronic control circuits; and
- Environmentally acceptable and recyclable materials.

Recent development activity in NiMH batteries has focused on further improvements in peak power for HEV and portable power tool applications. In this paper, we will report our results in raising power and high rate discharge capability, with particular emphasis to the metal hydride electrode surface catalytic activity at the metal/electrolyte oxide interface.

2. Experimental

Metal hydride alloys having formulas typified by $\text{V}_5\text{Ti}_9\text{Zr}_{26.2}\text{Ni}_{38}\text{Cr}_{3.5}\text{Co}_{1.5}\text{Mn}_{15.6}\text{Al}_{0.4}\text{Sn}_{0.8}$ (atomic %, a/o) and $\text{Ti}_8\text{Zr}_{29}\text{Ni}_{29}\text{Cr}_8\text{Co}_{11}\text{Mn}_{15}$ (a/o) were prepared by vacuum induction melting to have multiphase C14 and

*Corresponding author.

C15 structures. Alloy powder was produced by a single hydride/dehydride cycle and pulverization to below 75 μm . Electrodes were prepared by compacting or pasting the powder onto a copper expanded metal substrate using 0.5% PTFE binder.

C size cylindrical cells were assembled using a pasted style positive electrode consisting of $\text{NiCo}_5\text{Zn}_{0.5}\text{Ca}_{1.0}\text{Mg}_{0.5}$ active material (weight %) with high conductivity additives consisting of nickel metal fibers, cobalt and cobalt oxide [2].

The C cells were tested for power by comparing cell voltage and resistance at the C rate and 10C rate discharge using 10 s pulses as;

$$P_{\text{peak}} = 0.5 V_{\text{oc}} \times 0.5 I_{\text{max}}$$

AC impedance studies of the metal hydride electrode ($\sim 1.5 \text{ cm}^2$, $\sim 200 \text{ mg}$) were conducted in a flooded electrolyte, half cell configuration with respect to an Hg/HgO reference electrode. AC impedance measurements were performed using an EG&G 263A potentiostat and a Solatron SI1250 frequency response analyzer.

Analysis of the metal hydride surface was conducted by disassembly of discharged C cells in an argon glove box, with the metal hydride electrode rinsed and dried of KOH. Samples were prepared for examination by progressive polishing followed by dimple grinding to a specimen thickness of about 50 μm . The samples were then ion-milled at cryogenic temperature using 3–6 keV argon ions to a specimen thickness of about 500 \AA . Investigation of the MH surface oxide was performed on a JEOL-2010 scanning transmission electron microscope (STEM) using brightfield and darkfield imaging. Crystal structures were studied using selected area electron diffraction (SAED). Quantitative energy dispersive spectroscopy (EDS) analyses were obtained using a Cliff–Lorimer thin film correction procedure in conjunction with experimental X-ray correction factors (k-factors) obtained from thin film standards.

3. Results and discussion

3.1. Alloy design concept

NiMH batteries are an unusual battery technology in that the metal hydride active material is an engineered alloy made up of many different elements and that the MH alloy formulas vary to a significant degree [3]. Following the principles we have developed [4], disordered metal hydride materials based on transition, rare earth and magnesium alloys have been produced. The active material in the negative electrode is either of the disordered AB_5 (LaCePrNdNiCoMnAl) or disordered AB_2 (VTiZrNiCrCoMnAlSn) type, where the ‘ AB_x ’ designation refers to the ratio of the A type elements (LaCePrNd or

TiZr) to that of the B type elements (VNiCrCoMnAlSn). Disorder takes into account that elements containing both d and f orbitals can be used to produce multiphase materials having a spectrum of hydrogen binding energy with either type of element serving as a host matrix. In either case, commercial NiMH hydrogen storage materials have complex microstructures and operate in the aggressive environment (30% KOH electrolyte, oxygen gas in overcharge recombining at the MH surface) within the battery where most of the metals are thermodynamically more stable as oxides. AB_5 type alloys are more common, despite significantly lower hydrogen storage capacity as compared to AB_2 (320 vs. 440 mAh g^{-1}). Significant ongoing development has improved the properties of AB_2 materials such as cycle life, charge retention, and power to take advantage of the inherently higher energy that is especially important to reduce cost [5,6].

Electrochemical utilization of metal hydride materials as anodes in NiMH batteries requires meeting a demanding list of performance attributes including hydrogen storage capacity, suitable metal-to-hydrogen bond strength, acceptable catalytic activity and discharge kinetics, and sufficient oxidation/corrosion resistance to allow for long cycle life. Multielement, multiphase, disordered alloys of the LaNi_5 and VTiZrNiCr type are attractive development candidates for atomic engineering due to a broad range of elemental addition and substitution, availability of alternate crystallographic phases which form the matrix for chemical modification, and a tolerance for non-stoichiometric formulas. For example, practical multiphase AB_2 alloys may precipitate with microstructures containing one or more of C14 hexagonal, C15 cubic, FCC, and BCC crystallographic structures. Through the introduction of modifier elements, ease of activation and formation has been achieved. Special processing steps have been developed, such as alloy melting and size reduction suitable for these metallurgically challenging materials in terms of molten reactivity, degree of alloying, and high hardness.

The metal hydride active material and electrode construction also have similar special design options. The active materials may be adjusted to influence one or more of capacity, power, and/or cycle life. Disorder, by allowing multiphase microstructures and multiple lattice constants within a given crystallographic structure, permits an extra degree of alloy design flexibility and allows for a high level of chemical substitution. For the AB_5 system, a typical formula is $\text{La}_{5.7}\text{Ce}_{8.0}\text{Pr}_{0.8}\text{Nd}_{2.3}\text{Ni}_{59.2}\text{Co}_{12.2}\text{Mn}_{6.8}\text{Al}_{5.0}$ (atomic percent a/o). While the capacity of various AB_5 alloys is usually around 290–320 mAh g^{-1} , other overall performance attributes can be greatly influenced [7]. It is common for the ratio of La/Ce to be reversed to emphasize cycle life and power. The total amount of Co, Mn and Al significantly affect ease of activation and formation but increased cobalt has cost implications. After production of the AB_5 alloy ingot, it is common to further refine the microstructure of the material by a post anneal

treatment of perhaps 1000°C for 10 h. The annealing treatment can have a significant effect on capacity, discharge rate and cycle life by adjusting crystallite size and grain boundaries, as well as eliminating unwanted phases precipitated during ingot melting and casting [8,9]. Commercial AB₅ alloys have a predominantly CaCu₅ crystallographic structure. However, within that structure, there is a range of lattice constants brought about by compositional disorder within the material that are important to catalysis, storage capacity and stability to the alkaline environment and embrittlement [10]. These materials also precipitate a nickel–cobalt phase that is important to high rate discharge [11].

AB₂ alloys also have formula and processing choices. Popular AB₂ alloy formulas (a/o) include V₁₈Ti₁₅Zr₁₈Ni₂₉Cr₅Co₇Mn₈ and V₅Ti₉Zr_{26.2}Ni₃₈Cr_{3.5}Co_{1.5}Mn_{15.6}Al_{0.4}Sn_{0.8}.

Alloy capacity may range from 385 to 450 mAh g⁻¹. High vanadium content alloys may suffer from higher rates of self discharge due to the solubility of vanadium oxide and its consequent ability to form a special type of redox shuttle [12]. The concentration of Co, Mn, Al and Sn are important for easy activation and formation and long cycle life. The ratio of hexagonal C14 to cubic C15 phase is important to emphasize capacity or power [13,14].

3.2. Alloy and battery performance

NiMH specific energy can vary from 42 to 100 Wh kg⁻¹ depending on the particular application requirements. For laptop computers where run time is paramount, NiMH batteries need not have high power capability or even ultra-long cycle life. On the other hand, for extremely high power charge and discharge, extra current collection, high N/P ratios (proportion of excess negative electrode capacity to positive electrode capacity), and other cell design and construction decisions can additively affect specific energy. Fig. 1 presents NiMH specific energy improvements over the last 10 years in consumer (portable) cylindrical cells. For the most common small consumer NiMH batteries, specific energy is usually about 75–95

Wh kg⁻¹, for EV batteries usually about 65–80 Wh kg⁻¹, and for HEV batteries and other high power applications about 45–60 Wh kg⁻¹ [15]. While gravimetric energy usually receives the attention for advanced battery technologies, in many cases volumetric energy density in watt-hours per liter is actually more important. NiMH has exceptionally good energy density, achieving up to 320 Wh l⁻¹. Cost reduction is at the forefront of NiMH development. High volume consumer battery production has seen NiMH cost come at or below the \$/Wh cost of NiCd, previously thought to be unobtainable. NiMH cost reduction begins with the recognition that the technology cost is primarily materials intensive. Effort to raise specific energy involves development of metal hydride alloys with higher hydrogen storage capacity (from 320–385 mAh g⁻¹ active material to 450 mAh g⁻¹) and higher utilization nickel hydroxide (from 240 mAh g⁻¹ active material to 280–300 mAh g⁻¹). Each of these higher utilization active materials involves innovative materials research involving highly modified alloy formulas and advanced processing techniques.

While electric vehicles may use a battery of about 200 W kg⁻¹, hybrid electric vehicles are now becoming the prominent environmentally conscious vehicle approach. HEV applications require battery specific power in excess of 500 W kg⁻¹ and preferably 1000 W kg⁻¹. In addition, traditional lead-acid starting-lighting-ignition (SLI) batteries are problematic in size and weight when automotive requirements call for 42-volt electrical systems. NiMH batteries are considered the leading advanced battery for high voltage SLI applications due to the following advantages compared to lead-acid: higher gravimetric and volumetric energy and longer cycle life, especially under high depth of discharge. Ongoing work will include improving low temperature power at –30°C and initial cost at low to moderate production volumes.

3.3. MH surface oxide and catalysis

A critical design factor within the metal hydride surface oxide is to achieve a balance between surface oxide passivation and corrosion. Porosity within the oxide is important to allow ionic access to the metallic catalysts and therefore promote high rate discharge. While passivation of the oxide is problematic for high rate discharge and cycle life, unrestrained corrosion is equally destructive. Oxidation and corrosion of the anode metals consumes electrolyte, changes the state of charge balance by release of hydrogen in the sealed cell, and creates corrosion products which are capable of poisoning the positive electrode by causing premature oxygen evolution. Establishing a balance between passivation and corrosion for stability is a primary function of compositional and structural disorder.

For both AB₅ and AB₂ metal hydride alloys, the metal/

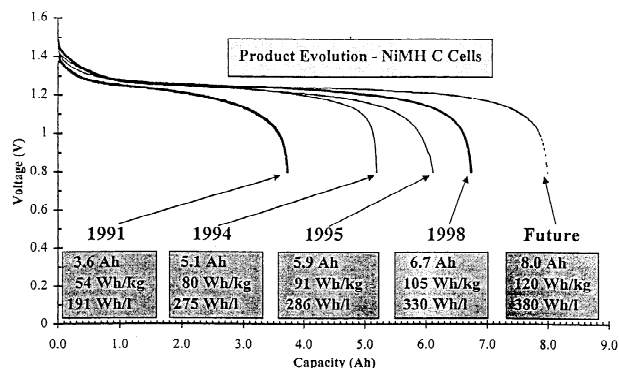


Fig. 1. Advances in NiMH technology specific energy.

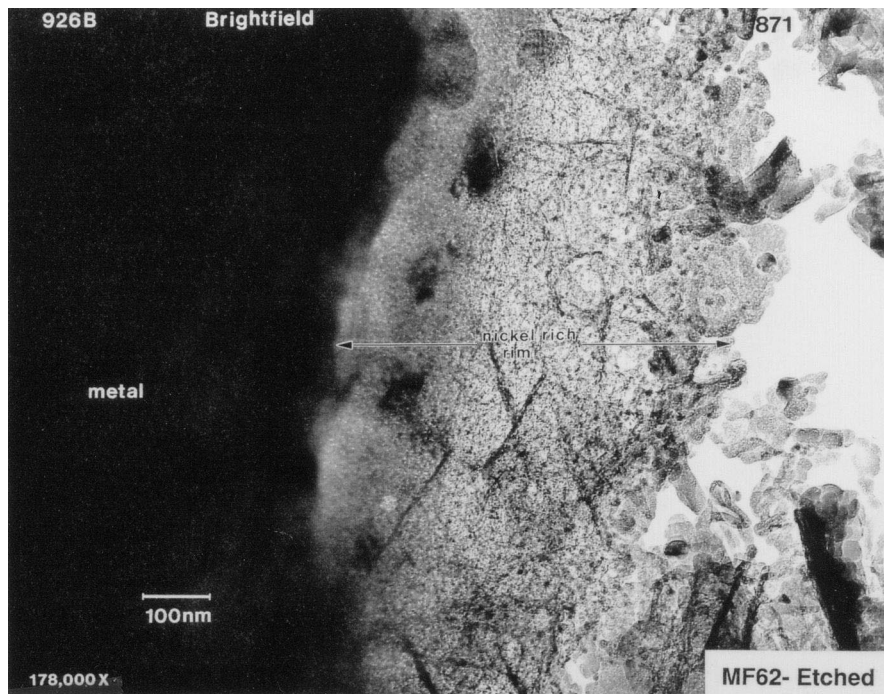


Fig. 2. TEM micrograph of VTiZrNiCrCoMnAlSn alloy surface oxide having high catalytic activity (brightfield imaging).

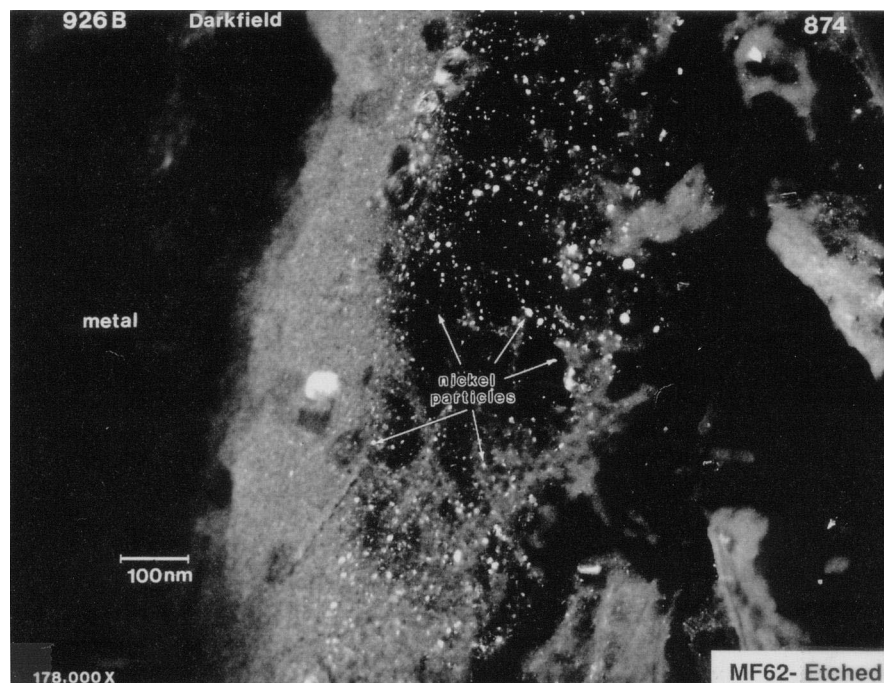


Fig. 3. TEM micrograph of VTiZrNiCrCoMnAlSn alloy surface oxide having high catalytic activity (darkfield imaging).

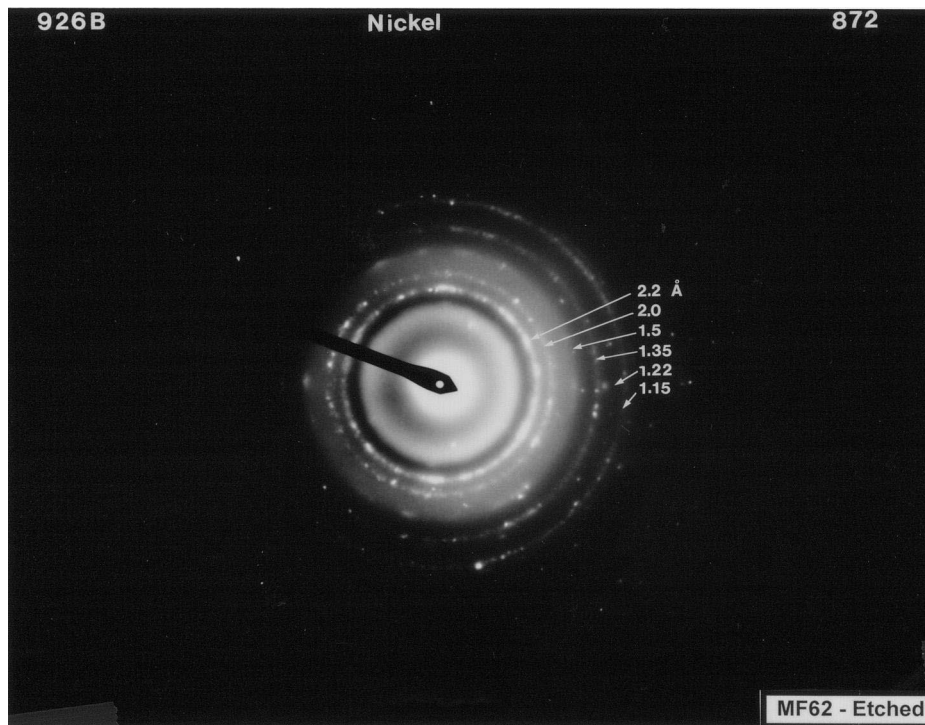


Fig. 4. Select area electron diffraction (SAED) pattern of VTiZrNiCrCoMnAlSn alloy surface oxide inclusions (Ni regions in Fig. 3).

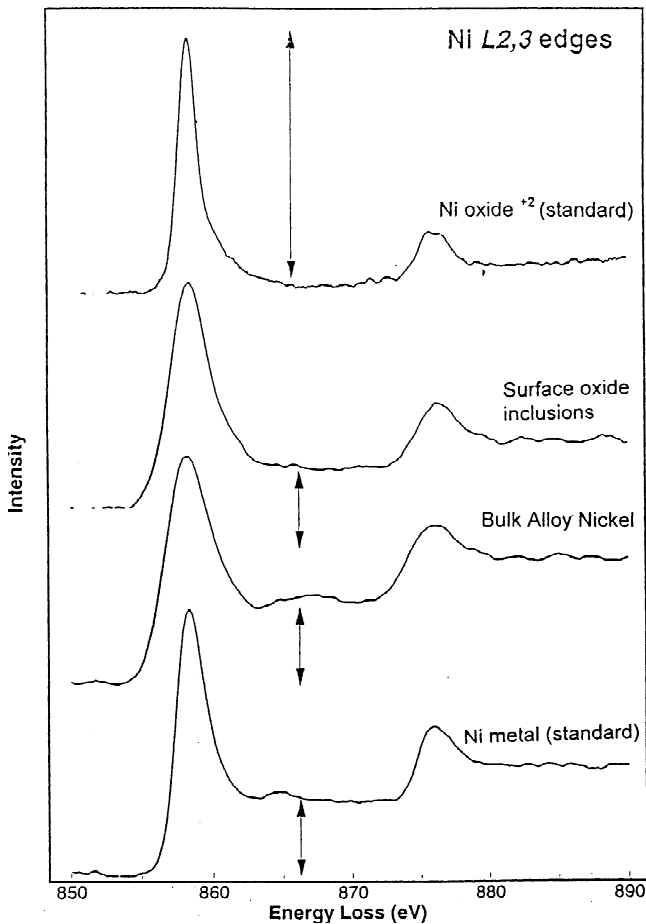


Fig. 5. Electron energy loss spectroscopy (EELS) of VTiZrNiCrCoMnAlSn alloy surface oxide having high catalytic activity.

electrolyte surface oxide interface is a crucial factor in discharge rate capability and cycle life stability [16–18]. Original LaNi_5 and TiNi alloys extensively studied in the 1970s and 1980s for NiMH battery applications were never commercialized due to poor discharge rate and cycle life capability [19–21]. Lack of catalytic activity at the surface oxide limits high rate discharge and lack of sufficient oxidation/corrosion resistance is a critical obstacle to long cycle life. The complicated chemical formulas and microstructures of present disordered AB_5 and AB_2 alloys extends to the surface oxide. At the oxide, important factors include thickness, microporosity and catalytic activity. In particular, the oxide interface between the metal hydride and the electrolyte has been identified as essential for low voltage loss under pulse discharge. Of crucial importance to discharge rate was the use of ultrafine metallic nickel alloy particles having a size less than 70 Angstroms dispersed within the oxide. These particles are excellent catalysts for the reaction of hydrogen and hydroxyl ions, and are especially important for reducing activation polarization [22].

The ultrafine metallic catalysts are created by preferential corrosion within the multielement hydrogen storage alloy. In particular, the dissolution and precipitation of the less noble vanadium, titanium and zirconium allow nickel in the presence of cobalt, manganese and aluminum to form the metallic clusters requires careful atomic engineering based on the lack of such proximity of nickel atoms in the unit cell. Once the concept of designed preferential corrosion was utilized, it becomes a simple matter to transfer the concept from the originally disclosed d band

materials to allow the finely divided surface catalysts within the disordered f band AB₅ alloy. The keys to success of the catalysts are size, number, density, and topology of the metallic particles. Nickel in the metallic state is electrically conductive and catalytically active. By further alloying the catalysts with cobalt (~20% a/o), the relative size of the catalysts can be reduced from about on average 50–70 Å to about 20–50 Å.

Disorder allows such finely divided metallic catalysts ('surface sites') by taking into account the entire spectrum of local order effects such as porosity, topology, catalyst size and proximity. While a tremendous amount of research investigates development of nanocrystalline materials, it is important to note that such materials exist at the surface interface of today's 900 million per year NiMH batteries. The catalyst size is important in that at less than 70 Å size, there are an approximately equivalent amount of surface atoms and bulk atoms. The close proximity of the metallic catalysts, typically about 100 Å apart, may also be referred to as 'density of sites'. It is the interaction of the local chemical electronic bonds with the reacting H⁺ and

OH⁻ that makes these catalysts so effective, and it is their metallic nature, size and number which provide excellent poisoning resistance.

The investigation of the MH surface oxide was conducted using a scanning transmission electron microscope having the capability for EDS, SAED and EELS [23]. Figs. 2 and 3 present high magnification brightfield and darkfield TEM images of the surface oxide exhibiting high catalytic activity. The bright inclusions under darkfield imaging are useful for determining the size of the catalyst and are indicative of very strong electron diffraction from nanocrystals having high crystallinity. Wide area EDS shows an enriched nickel surface to be expected from the preferential corrosion of the other base alloy constituents. Fine beam EDS of the inclusion shows almost no oxygen relative to a high nickel or nickel-cobalt peak intensity while the area surrounding the nickel inclusion is rich in oxygen. To provide further corroboration, SAED is presented in Fig. 4. Indexing of this ring pattern is consistent with metallic nickel rather than nickel oxide. Final support for our finding that the improved alloy catalytic activity is

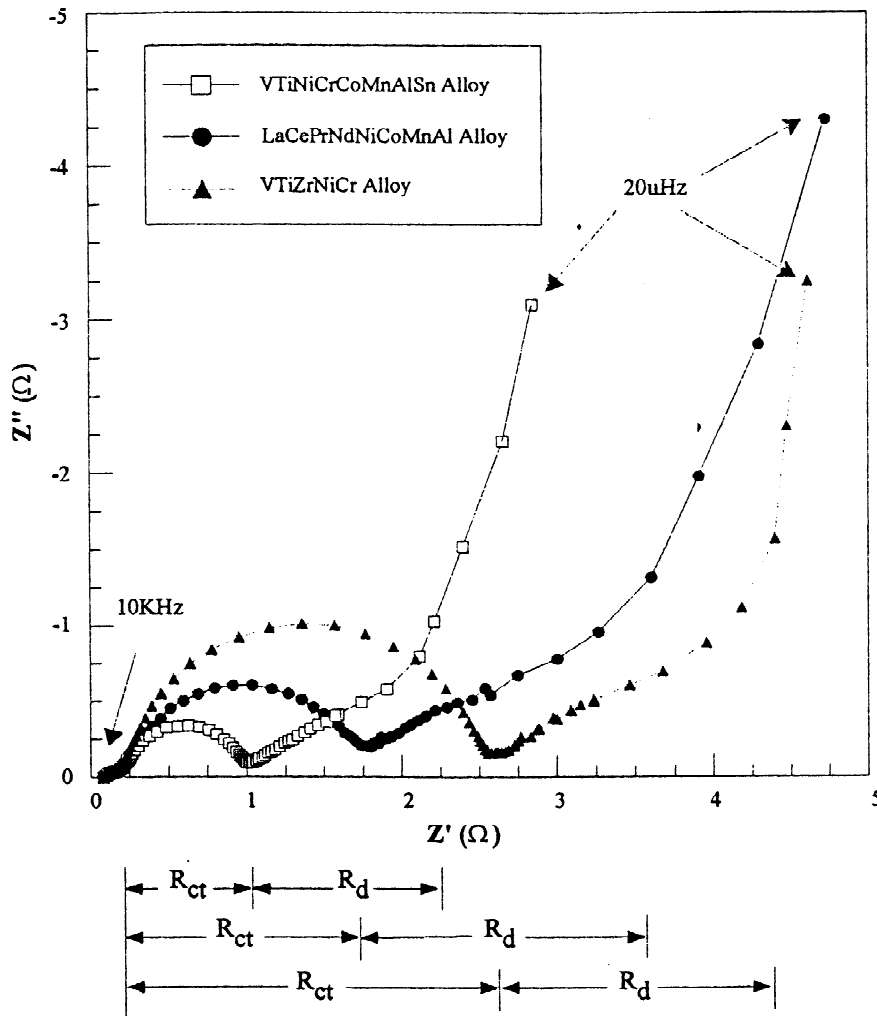


Fig. 6. AC impedance Nyquist analysis of metal hydride alloy catalytic activity (R_{ct} charge transfer resistance, R_d diffusion resistance).

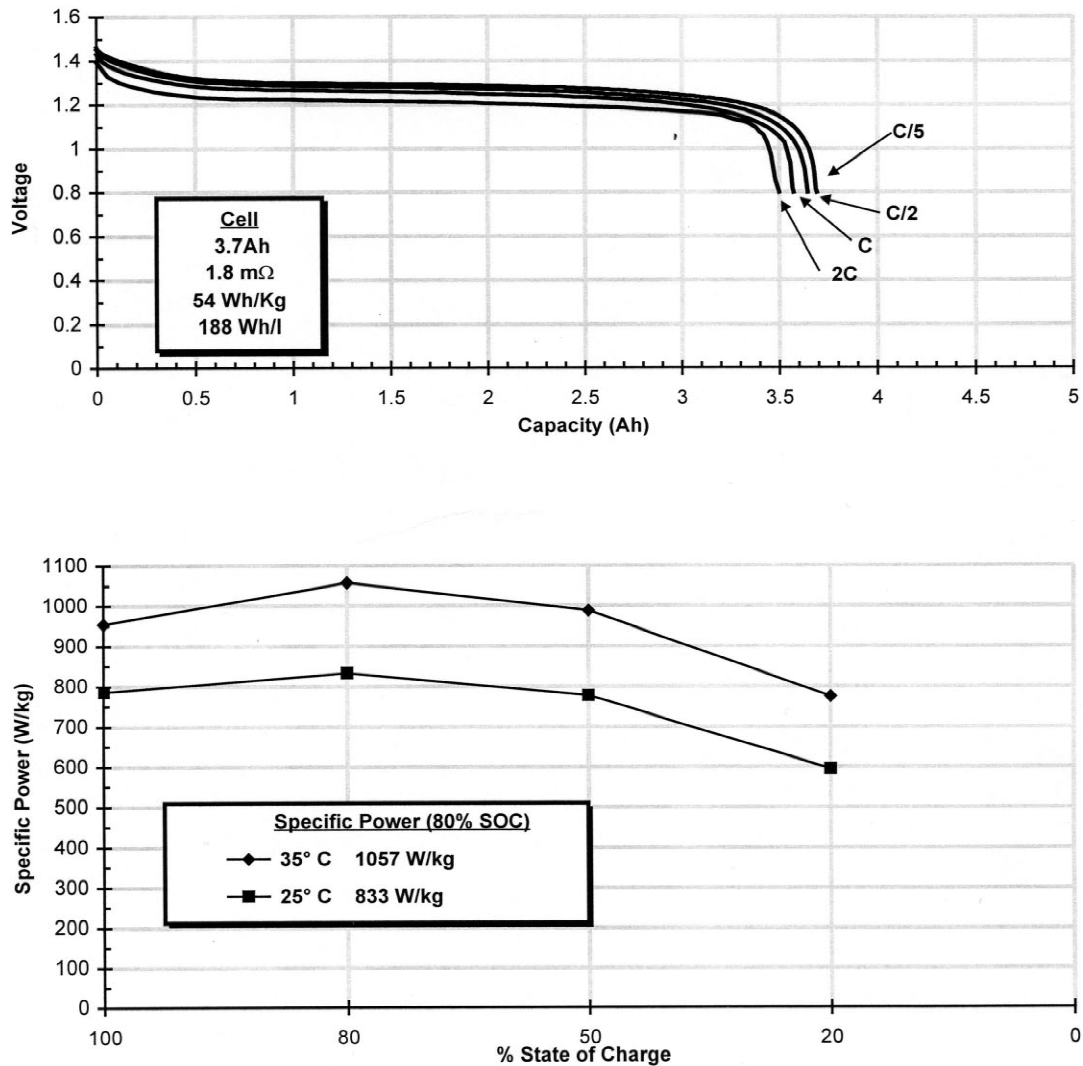


Fig. 7. NiMH C capacity and voltage under varying rate discharge (top) and specific power measured at C rate, 10C rate discharge using 10 s pulses (bottom).

the result of the MH surface oxide interface including the presence of the ultrafine metallic nickel inclusions was provided by EELS, where energy loss shows the inclusions to be at Ni^{+0} oxidation state (Fig. 5).

Comparable tests on earlier low catalytic activity MH materials showed the absence of inclusions within the oxide under darkfield imaging, a high oxygen signal throughout the oxide under EDS, SAED patterns characteristic of nickel oxide and EELS spectra indicative of nickel in the +2 oxidation state.

AC impedance measurements of the highly catalytic MH materials on a half-cell basis are presented in Fig. 6, where low frequency resistance measurements indicate a higher rate of hydrogen diffusion for hydride alloys having the surface oxide catalytic sites and the charge transfer resistance was two to three times smaller [24,25]. The resulting higher exchange current density of the surface modified

materials reflects the higher catalytic activity of the metal oxide surface interface with the electrolyte.

NiMH C cell and HEV batteries were assembled using the MH materials exhibiting the improved surface oxide. C cell specific power of 1057 W kg^{-1} at 35°C was achieved under the HEV required test conditions of 10 second pulses at a current of 10-C rate (40 Amps for a 4Ah C cell), as presented in Fig. 7. Typical commercial high power NiMH cylindrical cells have a specific power in the 600 W kg^{-1} range.

4. Conclusions

Specific power and high rate discharge of disordered hydrogen storage alloys for electrochemical application in NiMH batteries was significantly improved by combining

physics and chemistry in the design of the surface oxide on the metal hydride materials. By introducing extremely small diameter metallic nickel alloy inclusions throughout the oxide through the method of preferential corrosion, catalytic activity through reduced charge transfer resistance was significantly increased and a NiMH battery specific power of 1057 W kg^{-1} was attained.

References

- [1] S.R. Ovshinsky, S.K. Dhar, M.A. Fetcenko, K. Young, B. Reichman, C. Fierro, J. Koch, F. Martin, W. Mays, B. Sommers, T. Ouchi, A. Zallen, R. Young, in: 17th International Seminar & Exhibit on Primary and Secondary Batteries, Ft. Lauderdale, Florida, March 6–9, 2000.
- [2] M. Oshitani, H. Yufu, K. Takashima, S. Tsuji, Y. Matsumaru, J. Electrochem. Soc 136 (6) (1989).
- [3] S.R. Ovshinsky, M. Fetcenko, J. Ross, Science 260 (1993) 176.
- [4] S.R. Ovshinsky, in: D. Adler, B. Schwartz, M. Silver (Eds.), Disordered Materials: Science and Technology, Institute For Amorphous Studies Series, Plenum Publishing Corporation, New York, 1991.
- [5] H. Nakano, S. Wakao, J. Alloys Comp. 231 (1995) 587–593.
- [6] T. Gamo, Y. Tsuji, Y. Moriwaki, Proceedings of the Electrochemical Society, Hydrogen and Metal Hydride Batteries, 94-27, 1994, pp. 155–164.
- [7] M. Latroche, A. Percheron-Guegan, Y. Chabre, J. Bouet, J. Panetier, E. Ressouche, J. Alloys Comp. 231 (1995) 537–545.
- [8] T. Sakai, H. Miyamura, N. Kuriyama, H. Ishikawa, I. Uehara, J. Alloys Comp. 192 (1993) 155–157.
- [9] R. Mishima, H. Miyamura, T. Sakai, N. Kuriyama, H. Ishikawa, I. Uehara, J. Alloys Comp. 192 (1993) 176–178.
- [10] T. Weizhong, S. Guangfei, J. Alloys Comp. 203 (1994) 195–198.
- [11] P.H.L. Notten, J.L.C. Daams, R.E.F. Einerhand, Ber. Bunsenges. Phys. Chem 96 (5) (1992).
- [12] M.A. Fetcenko, S. Venkatesan, S. Ovshinsky, in: Proceedings of the Symposium on Hydrogen Storage Materials, Batteries, and Electrochemistry, Electrochemical Society, Pennington, NJ, 1992, p. 141.
- [13] H. Nakano, S. Wakao, T. Shimizu, J. Alloys Comp. 253–254 (1997) 609–612.
- [14] M. Bououdina, D.L. Sun, H. Enoki, E. Akiba, J. Alloys Comp. 288 (1999) 229–237.
- [15] R.C. Stempel, S.R. Ovshinsky, D.A. Corrigan, IEEE Spectrum 35 (11) (1998).
- [16] A. Zuttel, F. Meli, L. Schlapbach, J. Alloys Comp. 200 (1993) 157–163.
- [17] A. Zuttel, F. Meli, L. Schlapbach, J. Alloys Comp. 231 (1995) 157–163.
- [18] J.W. Kim, S.M. Lee, H.H. Lee, D.M. Kim, J.Y. Lee, J. Alloys Comp. 255 (1997) 248–252.
- [19] K. Beccu, in: United States Patent, Vol. 3,669,745, 1972.
- [20] J.R. van Beek, H.C. Donkersloot, J.J.G. Willems, in: Proceedings of the 14th International Power Sources Symposium, 1984.
- [21] M.A. Gutjahr, H. Buchner, K.D. Beccu, H. Saufferer, in: D.H. Collins (Ed.), Power Sources, Vol. 4, Oriel, Newcastle upon Tyne, United Kingdom, 1973, p. 79.
- [22] M.A. Fetcenko, S.R. Ovshinsky, B. Chao, B. Reichman, in: United States Patent, Vol. 5,536,591, 1996.
- [23] J.P. Bradley, D.A. Brooks, in: Analytical Electron Microscopy in Materials Science, American Laboratory, 1988.
- [24] B. Reichman, W. Mays, M.A. Fetcenko, S.R. Ovshinsky, in: Electrochemical Society Proceedings, Vol. 97-16, 1997.
- [25] B. Reichman, W. Mays, K. Young, M.A. Fetcenko, S.R. Ovshinsky, T. Ouchi, in: Electrochemical Society Proceedings, Vol. 98-15, 1998.